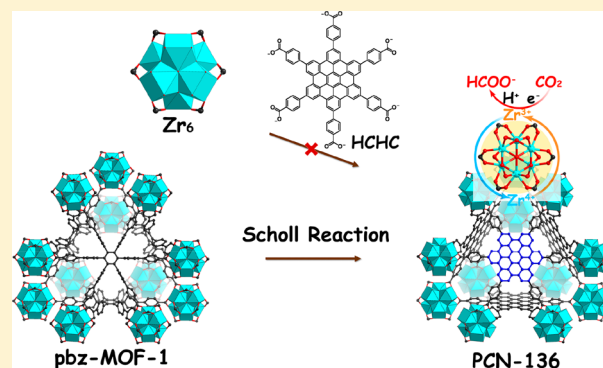


Creating Well-Defined Hexabenzocoronene in Zirconium Metal–Organic Framework by Postsynthetic Annulation

Jun-Sheng Qin,^{†,¶,□} Shuai Yuan,^{†,△,□} Lei Zhang,[§] Bao Li,^{†,□} Dong-Ying Du,[⊥] Ning Huang,^{†,□} Wei Guan,^{⊥,□} Hannah F. Drake,[†] Jiandong Pang,[†] Ya-Qian Lan,^{*,§,□} Ali Alsalmeh,^{*,‡} and Hong-Cai Zhou^{*,†,‡,□}[†]Department of Chemistry, Texas A&M University, College Station, Texas 77843-3255, United States[‡]Chemistry Department, College of Science, King Saud University, Riyadh 11451, Saudi Arabia[§]School of Chemistry and Materials Science, Nanjing Normal University, Nanjing 210023, P. R. China[⊥]Institute of Functional Material Chemistry and National & Local United Engineering Lab for Power Battery, Department of Chemistry, Northeast Normal University, Changchun 130024, P. R. China[¶]State Key Laboratory of Inorganic Synthesis and Preparative Chemistry, College of Chemistry, International Center of Future Science, Jilin University, Changchun 130012, P. R. China[△]Department of Mechanical Engineering, Department of Material Science and Engineering, Massachusetts Institute of Technology, Cambridge, Massachusetts 02139, United States

S Supporting Information

ABSTRACT: The incorporation of large π -conjugated ligands into metal–organic frameworks (MOFs) can introduce intriguing photophysical and electrochemical properties into the framework. However, these effects are often hindered by the strong π – π interaction and the low solubility of the arylated ligands. Herein, we report the synthesis of a porous zirconium-based MOF, $\text{Zr}_6(\mu_3\text{-O})_4(\mu_3\text{-OH})_4(\text{OH})_6(\text{H}_2\text{O})_6(\text{HCHC})$ (PCN-136, HCHC = hexakis(4-carboxyphenyl)hexabenzocoronene), which is composed of a hexacarboxylate linker with a π -conjugated hexabenzocoronene moiety. Direct assembly of the Zr^{4+} metal centers and the HCHC ligands was unsuccessful due to the low solubility and the unfavorable conformation of the arylated HCHC ligand. Therefore, PCN-136 was obtained from aromatization-driven postsynthetic annulation of the hexaphenylbenzene fragment in a preformed framework (pbz-MOF-1) to avoid π – π stacking. This postsynthetic modification was done through a single-crystal-to-single-crystal transformation and was clearly observable utilizing single-crystal X-ray crystallography. The formation of large π -conjugated systems on the organic linker dramatically enhanced the photoresponsive properties of PCN-136. With isolated hexabenzocoronene moieties as photosensitizers and Zr–oxo clusters as catalytic sites, PCN-136 was employed as an inherent photocatalytic system for CO_2 reduction under visible-light irradiation, which showed increased activity compared with pbz-MOF-1.



INTRODUCTION

In the past few decades, there has been an increase in consumption of fossil fuels which has resulted in increasing challenges to meet these energy demands and has strained current environmental resources. Therefore, the harvest of clean and sustainable solar energy caught considerable interdisciplinary attention for its great potential in energy and environmental applications.^{1–4} It is known that an increase in anthropogenic atmospheric carbon dioxide has contributed to global warming. A novel way to combat anthropogenic carbon dioxide and aid the fuel demand currently seen in our modern world is to synthesize fuels from the photocatalytic conversion of CO_2 . So far, many semiconductors have been explored as photocatalysts for CO_2 reduction, such as TiO_2 ,

CdS , and ZnS .^{5–7} Recently, metal–organic frameworks (MOFs)^{8,9} have been utilized as photocatalysts for CO_2 reduction,^{10–12} owing to their porosity for CO_2 absorption and ability to inherently contain visible-light-responsive moieties, thus avoiding the need for the introduction of a photosensitizer. MOFs are highly ordered crystalline porous materials which possess tunable porosity and designable functionalities that make them promising candidates for a variety of applications including gas capture and separation, sensor, and catalysis.^{13–22} For a material to be most effective as a visible-light photocatalyst, the most important feature that

Received: October 22, 2018

Published: January 9, 2019

the material must possess is the efficient harvest of a broad spectrum of visible light. When compared to the traditional inorganic semiconductors, the designable functionalization of MOFs with various visible-light-responsive fragments brings a unique opportunity for the development of heterogeneous photocatalysts. Consequently, the synthesis of a porous MOF which possesses a wide wavelength range of absorbable light may be a prime photocatalyst candidate for CO₂ reduction. To meet this challenge, several studies on MOF photocatalysts have been taken to expand the wavelength region of absorbing light, thus promoting their performance as catalysts.^{23–27} These reported MOFs were synthesized by the introduction of photoactive components (such as amine, porphyrin, and anthracene groups) and then applied for the visible-light-driven photoreduction of CO₂. Postsynthetic modification methods have been successfully employed for the introduction of desired functionalities into Zr-MOFs under relatively mild conditions.^{28–30} These methods have led to promising results in this field; however, it still remains a challenge to develop a new MOF system that can efficiently utilize the full solar spectrum (particularly >600 nm) for photocatalytic conversion of CO₂.

Graphene and graphitic carbon nitride (g-C₃N₄) have drawn increasing attention in the advancement of versatile photo-redox applications toward artificial photosynthesis. The properties that make these materials so favorable for these applications are their band structure, electronic properties, and optical absorption.^{31,32} Nanographenes in particular have size-dependent optical and redox properties and have been intensively explored as organic semiconductors in past decades owing to their extended conjugated π system.³³ The incorporation of extended π -conjugated systems into MOFs has the potential to combine the advantages of both systems. The framework of the MOF can serve to isolate the large π -conjugated fragment on the ligand, thus avoiding π – π interaction. The hindrance of the π – π interaction elongates the excitation state lifetime by suppressing the intramolecular charge transfer in the π -conjugated fragment. The crystalline MOF structure also allows for the arrangement of the large π -conjugated fragments into periodic arrays favoring light harvesting. Although there are clear benefits to the incorporation of large π -conjugated fragments into MOFs, the construction of large π -conjugated fragment-based MOF materials with well-defined structures remains largely unexplored. This can be attributed to the low solubility of the extended π -conjugated organic linkers which hindered the crystallization of the MOFs. Therefore, it is highly desirable to develop an effective method that can incorporate large π -conjugated fragments into stable porous MOF systems.

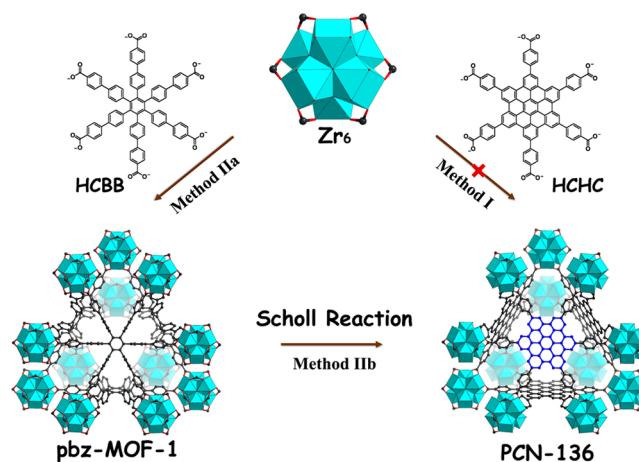
Herein, we report a hexabenzocoronene-based Zr-MOF, Zr₆(μ_3 -O)₄(μ_3 -OH)₄(OH)₆(H₂O)₆(HCHC) (PCN-136, HCHC = hexakis(4-carboxyphenyl)hexabenzocoronene), obtained from aromatization-driven postsynthetic annulation of the hexaphenylbenzene fragment in a preformed framework (pbz-MOF-1). The successful generation of hexabenzocoronene in a porous crystalline framework was confirmed by single-crystal X-ray diffraction, powder X-ray diffraction (PXRD), and nitrogen sorption experiments. Furthermore, the photocatalytic CO₂ reduction behaviors of PCN-136 and pbz-MOF-1 were investigated under visible-light irradiation in order to compare their photocatalytic performance derived from their organic fragments in the presence or absence of extended π -conjugated units. The hexabenzocoronene core in

PCN-136 behaves as a visible-light-harvesting unit, exhibiting enhanced photocatalytic efficiency compared with pbz-MOF-1 (hexaphenylbenzene core).

RESULTS AND DISCUSSION

Structural Design. The incorporation of π -conjugated fragment may enlarge the wavelength range of absorbable light and thus improve the photocatalytic performance. However, there is no accurate comparative model for this in the MOF system. We intend to employ MOFs with the same framework but in the presence or absence of large π -conjugated moieties. This approach is to investigate the influence of structure upon the photocatalytic property of the system. In this context, we attempted to produce a Zr-MOF starting from the combination of Zr(IV) precursors and a hexatopic carboxylate linker containing a π -conjugated hexabenzocoronene fragment, HCHC, through a one-pot synthetic approach. However, the direct assembly of the system failed to generate crystalline materials under the conventional conditions for the preparation of Zr-MOFs (Scheme 1, Method I). This is due to the

Scheme 1. Schematic View of the Preparation for PCN-136



strong π – π interaction between hexabenzocoronene moieties, which resulted in low solubility and hindered the crystallization of MOFs. In order to successfully synthesize the Zr-MOF in high crystallinity, a different synthetic route was taken.

To combat π – π stacking, a stepwise synthetic method was proposed. In polymer chemistry, the aromatization-driven annulation was commonly utilized to construct π -conjugated polymers.³⁴ It has also been used by the Hupp group as a postsynthetic modification method in the MOF system.³⁵ Bearing this in mind, we designed a stepwise synthetic route to introduce the large π -conjugated fragment into robust Zr-MOFs (Scheme 1, Method II). In this method, pbz-MOF-1 was initially synthesized by the solvothermal reaction of Zr⁴⁺ salt and hexakis(4'-carboxy[1,1'-biphenyl]-4-yl)benzene (noted as HCBP) following the literature (Figure S1).³⁶ Then, the intramolecular oxidative cyclodehydrogenation, or Scholl reaction,³⁷ was carried out using FeCl₃ as a catalyst.³⁸ By incubating the as-synthesized pbz-MOF-1 in the solution of FeCl₃/CH₂Cl₂, the hexaphenylbenzene core of the HCBP ligand within pbz-MOF-1 was transformed into a planarized hexabenzocoronene, giving rise to PCN-136 (Figure S2). Ultimately, PCN-136, a porous π -conjugated hexabenzocoronene-based Zr-MOF, was successfully produced through

chemical modification of the organic linker. It should be noted that PCN-136 and pbz-MOF-1 possess the same topological framework with the only difference in the structures being the central core units (the hexaphenylbenzene moiety in HCBB and the extended π -conjugated hexabenzocoronene in HCHC, respectively).

Single-Crystal-to-Single-Crystal Transformation. Due to the high chemical stability of Zr-MOFs, the aromatization-driven postsynthetic annulation of pbz-MOF-1 occurred in a single-crystal-to-single-crystal transformation. As such, the generation of hexabenzocoronene can be clearly observed by single-crystal X-ray crystallography. Single-crystal X-ray analysis revealed that PCN-136 crystallized in the cubic space group *Fd-3m* (No. 227, Table S1). The framework of PCN-136 consists of hexagonal Zr_6 clusters and hexabenzocoronene-based HCHC linkers (Figure 1a, b). A tetrahedral cavity of

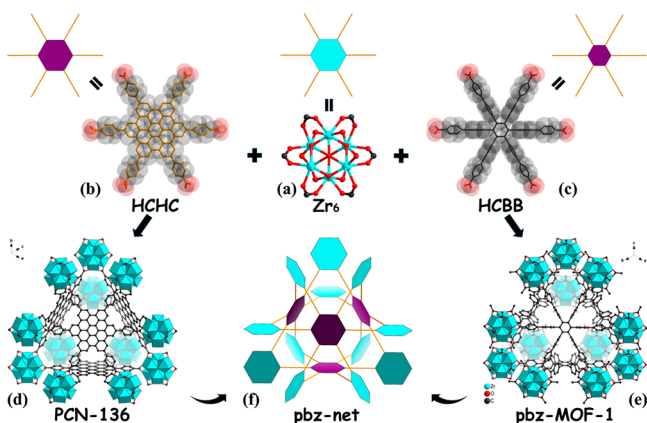


Figure 1. Structural comparison between PCN-136 and pbz-MOF-1: (a–c) the structures of Zr_6 cluster, HCHC, and HCBB as six-connected nodes and (d, e) the 3D structures and (f) pbz-net.

~ 15.5 Å in diameter exists in the structure of PCN-136 (Figure S3), which is delimited by 12 Zr_6 clusters (every 3 Zr_6 clusters acting as a vertex of the tetrahedron) and 4 organic linkers (serving as the faces of the tetrahedron). The solvent-accessible volume in PCN-136 calculated from PLATON software is estimated to be 74%.³⁹ From the topological viewpoint, each hexagonal Zr_6 cluster is regarded as a six-connected node, and each hexagonal flat hexabenzocoronene-based organic fragment is a six-connected linker. The resulting framework can be assigned into the default 6-c hgx topology (polybenzene-type (pbz) structure, Figure 1d, f). PCN-136 possesses the same topology as pbz-MOF-1 derived from the similar connectivity mode of organic linkers (Figure 1c, e), with the only difference being the central core units (the hexaphenylbenzene moiety in HCBB and the extended π -conjugated hexabenzocoronene in HCHC, respectively, Figure S4). Further careful structural analysis of PCN-136 indicated that the dihedral angle between the hexagonal plane of the Zr_6 cluster and the central hexabenzocoronene ring of the organic linker is 70.53° . As expected, the dihedral angle between two phenyl rings is 70.5° . Meanwhile, the complementary dihedral angles among the neighboring hexagonal rings derived from the Zr_6 clusters attached to the same hexagonal ring of the organic linker are 70.5° and 109.5° .

The PXRD pattern of the as-synthesized samples matches well with the simulated pattern (Figure S5), indicating the phase purity of PCN-136. In addition, PCN-136 was

characterized by thermalgravimetric and infrared (IR) spectra analysis (Figures S6 and S7). The architectural stability and permanent porosity of PCN-136 were confirmed by nitrogen adsorption–desorption measurement at 77 K with a reversible type-I isotherm feature (Figure S8a). The result suggests that PCN-136 is highly porous with a BET (Langmuir) surface area of $1768 \text{ m}^2 \cdot \text{g}^{-1}$ ($2009 \text{ m}^2 \cdot \text{g}^{-1}$). The pore volume of PCN-136 calculated at $0.95 P/P_0$ is $0.73 \text{ cm}^3 \cdot \text{g}^{-1}$. The pore size was calculated to be 15 Å from the nitrogen adsorption isotherm. This is consistent with the pore size determined from crystallographic analysis (Figure S8b). For comparison, the N_2 sorption isotherm of pbz-MOF-1 was also performed at 77 K (Figure S9). The BET surface area and pore volume of pbz-MOF-1 are similar to those of PCN-136. As shown in Figure S10, carbon dioxide adsorption–desorption isotherms of PCN-136 at 273 K were measured. Carbon dioxide uptake was as high as $61.01 \text{ cm}^3 \cdot \text{g}^{-1}$ at saturation. This result suggests that the interactions between sp^2 -bonded carbon atoms from the hexabenzocoronene fragments and CO_2 molecules may play an important role in the carbon dioxide uptake.^{40,41} In a previous computational study, the utilization of hexabenzocoronene unit as a central part of the linker resulted in a significant enhancement of the uptake of gases for the entire family of MOFs in the study.⁴² The successful construction of PCN-136 provides a platform for the comparison of structure-dependent photocatalytic performance between PCN-136 and pbz-MOF-1.

Photoelectrochemical Properties. As suggested by the UV–vis data results, PCN-136 exhibits a broad-band absorption covering the whole UV–visible-light region (Figure 2a). This feature is desirable for photocatalytic applications. However, the visible-light absorption of pbz-MOF-1 is only up to ~ 450 nm (Figure 2a). The optical absorption of PCN-136 shows large broadening compared to the free ligand HCHC (Figure S11). This difference is mainly derived from the aggregation of the HCHC ligands in the framework on the basis of fluorescence results (Figure S12). These results suggested that the electrons of PCN-136 can be more easily promoted to an excited state upon the visible-light irradiation when compared to free HCHC or pbz-MOF-1. Furthermore, density functional theory (DFT) calculations were performed to study the possible difference in the optical bandgap in pbz-MOF-1 and PCN-136 that may have resulted from the π -conjugated organic fragments. As shown in Figure S13, the frontier molecular orbital distributions for organic linkers (HCBB and HCHC) in pbz-MOF-1 and PCN-136 are presented. The highest occupied molecular orbital (HOMO) in HCBB is mainly delocalized over the exterior biphenyl carboxylic acid fragments, while the lowest unoccupied molecular orbital (LUMO) is delocalized over both the central benzene ring and the exterior biphenyl carboxylic acid fragments. The HOMO in the HCHC ligands mostly delocalizes over the central π -conjugated hexabenzocoronene unit, while the LUMO is formally delocalized over both the central π -conjugated hexabenzocoronene unit and the terminal benzoic acid fragments. It can be clearly seen that more extended conjugation generally leads to a smaller HOMO–LUMO gap (4.26 eV for HCBB vs 3.32 eV for HCHC). This accordingly enhances the degree of charge transfer from the ground state to the excited state. The DFT calculations confirm that the MOFs containing larger π -conjugated fragments would be more efficient for the utilization of the solar spectrum with similar metal nodes and frameworks. In

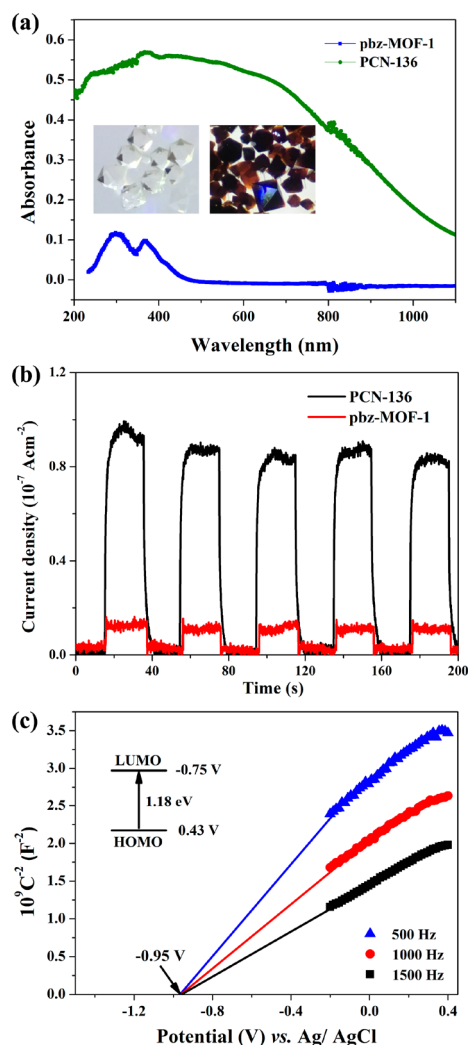


Figure 2. (a) UV-vis spectra of pbz-MOF-1 and PCN-136; insets are the optical pictures of pbz-MOF-1 (left) and PCN-136 (right). (b) Transient photocurrent responses of pbz-MOF-1 and PCN-136 in 0.5 M Na_2SO_4 aqueous solution under visible-light irradiation. (c) Mott-Schottky plots for PCN-136 in 0.2 M Na_2SO_4 aqueous solution; inset is the energy diagram of the HOMO and LUMO levels of PCN-136.

addition, the photocurrent profiles of PCN-136 and pbz-MOF-1 also indicated that PCN-136 is more active than pbz-MOF-1 under visible-light illumination (Figure 2b). The replacement of the central phenyl core in pbz-MOF-1 with the hexabenzocoronene moiety in PCN-136 did not lead to a significant change in the structural feature, but the optical absorption ability was greatly tuned. It is postulated from this result that the presence of a flat hexabenzocoronene central core will improve the light harvesting of a desired MOF. With this in mind, the use of HCHC linkers can be shown to endow PCN-136 with light-harvesting capabilities in order to be utilized as a suitable platform for photocatalytic studies.

The Mott-Schottky measurements on PCN-136 and pbz-MOF-1 were performed at a frequency of 500, 1000, and 1500 Hz, in order to elucidate their semiconductor characters and the possibility for the subsequent CO_2 photoreduction study. As shown in Figures 2c and S14, the positive slope of the obtained C^{2-} values (vs the applied potentials) is consistent with those of typical n-type semiconductors. The intersection points are independent of the frequency, and the flat-band

position of PCN-136 is determined from the intersection to be $\sim -0.95 \text{ V}$ vs Ag/AgCl (i.e., -0.75 V vs normal hydrogen electrode (NHE)). Generally, the bottom of the conduction band (LUMO) in n-type semiconductors can be determined to be approximately equal to the flat-band potential.⁴³ According to this, the LUMO of PCN-136 is estimated to be -0.75 V vs NHE. The optical bandgap of PCN-136 was calculated to be 1.18 eV based on the UV-vis spectrum (Figure S15), and its valence band (HOMO) was estimated to be 0.43 V vs NHE (Figure 2c). Given the much more negative potential of the LUMO in PCN-136 than the reduction potential for the conversion of CO_2 to formate, it is theoretically feasible for the photocatalytic reduction of CO_2 to generate formate to be accomplished utilizing PCN-136 as a catalyst. Furthermore, the Mott-Schottky plots suggest that pbz-MOF-1 can be employed as a visible-light-harvesting material utilizing the same method (Figure S14).

Photocatalytic CO_2 Reduction. Considering the permanent porosity, broad optical absorption, and semiconductor characteristics exhibited by PCN-136, the photocatalytic reduction of carbon dioxide over PCN-136 was further evaluated in the presence of triisopropanolamine (TIPA) as a sacrificial agent under visible-light irradiation. Similarly, TIPA was employed in the reaction serving as an electron donor and hydrogen donor to recycle the catalytic process like the role of triethanolamine (TEOA). Moreover, TIPA is a milder alkaline medium when compared to TEOA. In order to determine the optimized catalytic experimental conditions, the photocatalytic conversion reaction was conducted over a wide variety of experimental conditions (Figure S16). The concentration of HCOO^- was detected and quantitatively analyzed by in situ ion chromatography. HCOO^- anions were continuously produced and analyzed as time increased for the reaction. Remarkably, PCN-136 shows a higher photocatalytic activity for carbon dioxide reduction in a mixed $\text{MeCN}/\text{H}_2\text{O}$ system than in a single solvent. No other products can be detected in the gas and liquid phases, suggesting that the catalyst is highly selective toward the conversion. No HCOO^- was detected in the absence of PCN-136, demonstrating the critical role of the photocatalyst in the reaction. Moreover, no HCOO^- was generated when the reaction was carried out in the dark, demonstrating a truly photocatalytic process. A total amount of $10.52 \mu\text{mol}$ formate anions was produced within 12 h in the mixed solvents of acetonitrile (40 mL) and water (5 mL) in the presence of TIPA (5 mL) under continuous visible-light illumination. According to the above results, the following photocatalytic reduction of CO_2 was carried out in the presence of TIPA (5 mL) in a mixed solvent systems ($\text{CH}_3\text{CN}/\text{H}_2\text{O}$, v:v (mL) = 40:5) under Xe light (300 W, $\lambda \geq 420 \text{ nm}$). For comparison, HCHC was also used as a catalyst for CO_2 photoreduction under similar conditions. However, HCHC has no activity on CO_2 photoreduction (Figure S17), suggesting that the photocatalytic activity can be greatly improved by assembling the HCHC linkers into MOFs. Furthermore, pbz-MOF-1 was studied as the photocatalyst under the same conditions, and the amount of HCOO^- anion produced was only $3.53 \mu\text{mol}$ after 12 h (Figure 3a). The turnover numbers of PCN-136 and pbz-MOF-1 are 1.12 and 0.40, respectively, suggesting that the HCOO^- yield of PCN-136 is nearly 3 times higher than that of pbz-MOF-1 under the same reaction conditions. The results suggest that PCN-136 is superior to pbz-MOF-1 for applications as an active photocatalytic material in the conversion of CO_2 to HCOO^- under

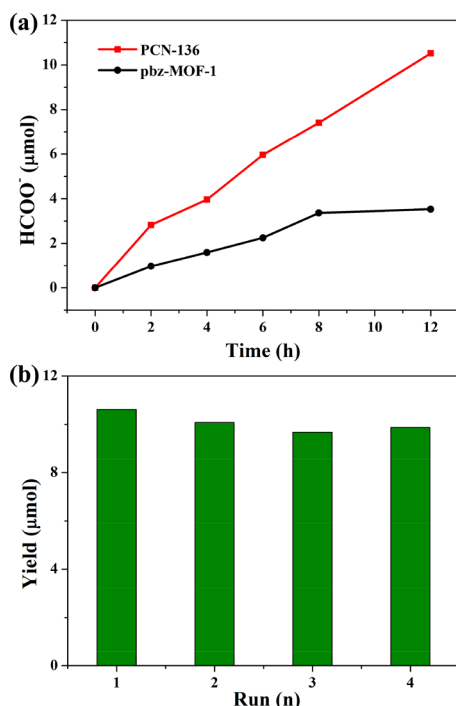


Figure 3. (a) Amount of HCOO⁻ produced as a function of irradiation time with PCN-136 or pbz-MOF-1 as photocatalysts (20 mg). MeCN/H₂O/TIPA (40/5/5 mL), Xe light (300 W, $\lambda \geq 420$ nm). (b) The amount of HCOO⁻ produced in four repeated photocatalytic reactions using PCN-136 as catalysts.

visible-light irradiation. The presence of extended π -conjugated hexabenzocoronene-based linkers in PCN-136 not only improves the optical absorption of the materials but also largely increases the yield of the photocatalytic reaction. As a comparison, Ru(bpy)₃Cl₂ (bpy = 2,2'-bipyridine) was introduced into the pbz-MOF-1 (20 mg) system as the photosensitizer with an amount of 11.2 mg (15 μmol) under similar conditions (Figure S18). Under these conditions, the amount of HCOO⁻ anion produced from pbz-MOF-1 increased from 3.53 μmol after 12 h to 11.11 μmol in 12 h, which is comparable to that of PCN-136. These results demonstrate that PCN-136 is very active and capable of selectively converting CO₂ to HCOO⁻ under visible-light irradiation. PCN-136 exhibits one of the highest performances of visible-light-driven CO₂ photoreduction to formate among reported MOFs or crystalline photocatalysts.^{25,27} In addition, PCN-136 can be easily separated and recovered from the reaction media by centrifugation for continued use. The recycling performance of the material was further investigated to examine the stability of PCN-136. The results of the cycling performance suggested that no obvious change in the yield rate of HCOO⁻ occurred during the four continuous runs (Figure 3b). After the photocatalytic experiments, the PXRD pattern was analyzed demonstrating that the structure of PCN-136 was maintained after reaction cycling (Figure S5).

Proposed Mechanism. After careful analysis of the results of the experiments, a reasonable mechanism can be proposed for the explanation of the CO₂ photoreduction over the PCN-136 (Figure 4). When the reaction system is irradiated, HCHC plays a role in absorbing visible light. Meanwhile, electrons are generated and transferred to the Zr^{IV}-oxo clusters, reducing the metal centers from Zr^{IV} to Zr^{III}. The intermediate Zr^{III} as the reactive site then reduces CO₂ to HCOO⁻ and is oxidized

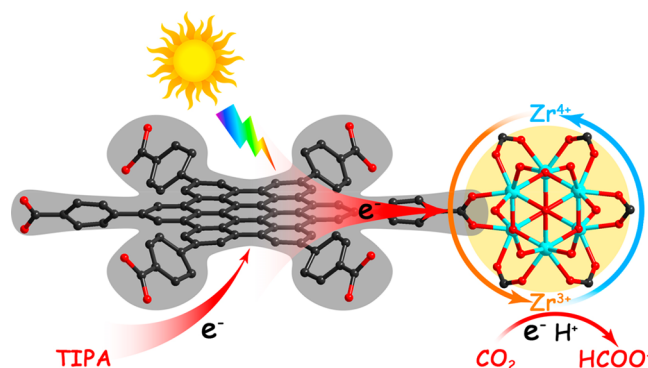


Figure 4. Plausible mechanism for photocatalytic CO₂ reduction over PCN-136 under visible-light irradiation.

back to Zr^{IV}. TIPA behaves as the electron donor to expend the photoinduced holes and achieve a complete photocatalytic reaction. A similar mechanism was proposed in previous work.^{25,44} Considering the similarity in topological framework, pore size distribution, active surface area, crystallinity, and particle size distribution of PCN-136 and pbz-MOF-1, it is noteworthy that the π -conjugated hexabenzocoronene-based organic fragment in PCN-136 contributes largely to the broadening of the range of absorbing visible light and thus enhances the photocatalytic activity of the MOF. MOFs, representing a new class of fascinating materials with great potential in the area of photocatalysts, hold great promise through the tunability of the porous structures and chemical compositions and the functionalization of porous environments at the molecular level. Integrating more required functions for heterogeneous catalysts into one single MOF material is fascinating and expected.

CONCLUSIONS

In summary, a π -conjugated hexabenzocoronene-based Zr-MOF, PCN-136, was obtained from aromatization-driven postsynthetic annulation of the hexaphenylbenzene fragment in a preformed framework, pbz-MOF-1. PCN-136 is highly efficient for visible-light-driven carbon dioxide reduction to produce formate. Specifically, PCN-136 exhibits a photocatalytic activity of three times that of pbz-MOF-1. These two structures have similar metal cluster, topological framework, pore size distribution, crystallinity, and particle size, but their catalytic performance is very different. The presence of a π -conjugated hexabenzocoronene core in the framework of PCN-136 plays a vital role in the improvement of the optical absorption properties of the material and also enhances the photocatalytic performance. The present work not only demonstrates a successful MOF model to study the structure-dependent photocatalytic performance but also provides solid experimental basis on the accurate design of heterogeneous photocatalysts at the molecular level. Furthermore, the aromatization-driven annulation is expected to become a versatile method for the incorporation of various π -conjugated systems in MOFs for advanced applications.

ASSOCIATED CONTENT

Supporting Information

The Supporting Information is available free of charge on the ACS Publications website at DOI: 10.1021/jacs.8b11042.

X-ray crystallographic details of the structure (CIF)

Text and tables giving experimental procedures for the preparation of PCN-136, photocatalytic CO₂ reduction, calculation details, PXRD patterns, gas adsorption isotherms, and other additional information (PDF)

AUTHOR INFORMATION

Corresponding Authors

*yqlan@njnu.edu.cn

*aalsalme@ksu.edu.sa

*zhou@chem.tamu.edu

ORCID

Bao Li: 0000-0003-1154-6423

Ning Huang: 0000-0002-7021-8705

Wei Guan: 0000-0001-7000-0274

Ya-Qian Lan: 0000-0002-2140-7980

Hong-Cai Zhou: 0000-0002-9029-3788

Author Contributions

□ These authors contributed equally.

Notes

The authors declare no competing financial interest.

ACKNOWLEDGMENTS

This work was supported by the Center for Gas Separations, an Energy Frontier Research Center funded by the U.S. Department of Energy, Office of Science, Office of Basic Energy Sciences (DE-SC0001015). The authors also acknowledge the financial supports from the National Natural Science Foundation of China (Grant No. 21621001) and the 111 Project (Grant No. B17020). The authors also acknowledge the financial supports from U.S. Department of Energy, Office of Fossil Energy, National Energy Technology Laboratory (DE-FE0026472) and National Science Foundation Small Business Innovation Research (NSF-SBIR) under Grant No. 1632486. This work was also funded by the Robert A. Welch Foundation through a Welch Endowed Chair to H.J.Z. (A-0030). The Distinguished Scientist Fellowship Program (DSFP) at KSU and National Science Foundation Graduate Research Fellowship (DGE: 1252521) are gratefully acknowledged. S.Y. also acknowledges the Dow Chemical Graduate Fellowship.

REFERENCES

- (1) Bard, A. J.; Fox, M. A. Artificial Photosynthesis: Solar Splitting of Water to Hydrogen and Oxygen. *Acc. Chem. Res.* **1995**, *28* (3), 141–145.
- (2) Zou, Z.; Ye, J.; Sayama, K.; Arakawa, H. Direct splitting of water under visible light irradiation with an oxide semiconductor photocatalyst. *Nature* **2001**, *414* (6864), 625–627.
- (3) Kubacka, A.; Fernández-García, M.; Colón, G. Advanced Nanoarchitectures for Solar Photocatalytic Applications. *Chem. Rev.* **2012**, *112* (3), 1555–1614.
- (4) Zhang, H.; Liu, G.; Shi, L.; Liu, H.; Wang, T.; Ye, J. Engineering coordination polymers for photocatalysis. *Nano Energy* **2016**, *22*, 149–168.
- (5) Inoue, T.; Fujishima, A.; Konishi, S.; Honda, K. Photoelectrocatalytic reduction of carbon dioxide in aqueous suspensions of semiconductor powders. *Nature* **1979**, *277* (5698), 637–638.
- (6) Fujiwara, H.; Hosokawa, H.; Murakoshi, K.; Wada, Y.; Yanagida, S.; Okada, T.; Kobayashi, H. Effect of Surface Structures on Photocatalytic CO₂ Reduction Using Quantized CdS Nanocrystals. *J. Phys. Chem. B* **1997**, *101* (41), 8270–8278.

- (7) Inoue, H.; Moriwaki, H.; Maeda, K.; Yoneyama, H. Photo-reduction of carbon dioxide using chalcogenide semiconductor microcrystals. *J. Photochem. Photobiol., A* **1995**, *86* (1–3), 191–196.
- (8) Zhou, H. C.; Long, J. R.; Yaghi, O. M. Introduction to Metal-Organic Frameworks. *Chem. Rev.* **2012**, *112* (2), 673–674.
- (9) Zhou, H. C.; Kitagawa, S. Metal-Organic Frameworks (MOFs). *Chem. Soc. Rev.* **2014**, *43* (16), 5415–5418.
- (10) Zhang, T.; Lin, W. B. Metal-organic frameworks for artificial photosynthesis and photocatalysis. *Chem. Soc. Rev.* **2014**, *43* (16), 5982–5993.
- (11) Qin, J. S.; Yuan, S.; Lollar, C.; Pang, J.; Alsalmeh, A.; Zhou, H. C. Stable metal-organic frameworks as a host platform for catalysis and biomimetics. *Chem. Commun.* **2018**, *54* (34), 4231–4249.
- (12) Lei, Z.; Xue, Y.; Chen, W.; Qiu, W.; Zhang, Y.; Horike, S.; Tang, L. MOFs-Based Heterogeneous Catalysts: New Opportunities for Energy-Related CO₂ Conversion. *Adv. Energy Mater.* **2018**, *8* (32), 1801587.
- (13) Sumida, K.; Rogow, D. L.; Mason, J. A.; McDonald, T. M.; Bloch, E. D.; Herm, Z. R.; Bae, T. H.; Long, J. R. Carbon Dioxide Capture in Metal-Organic Frameworks. *Chem. Rev.* **2012**, *112* (2), 724–781.
- (14) Sato, H.; Kosaka, W.; Matsuda, R.; Hori, A.; Hijikata, Y.; Belosludov, R. V.; Sakaki, S.; Takata, M.; Kitagawa, S. Self-Accelerating CO Sorption in a Soft Nanoporous Crystal. *Science* **2014**, *343* (6167), 167–170.
- (15) He, Y. B.; Zhou, W.; Qian, G. D.; Chen, B. L. Methane storage in metal-organic frameworks. *Chem. Soc. Rev.* **2014**, *43* (16), 5657–5678.
- (16) Du, D. Y.; Qin, J. S.; Li, S. L.; Su, Z. M.; Lan, Y. Q. Recent advances in porous polyoxometalate-based metal-organic framework materials. *Chem. Soc. Rev.* **2014**, *43* (13), 4615–4632.
- (17) Hu, Z. C.; Deibert, B. J.; Li, J. Luminescent metal-organic frameworks for chemical sensing and explosive detection. *Chem. Soc. Rev.* **2014**, *43* (16), 5815–5840.
- (18) Qin, J. S.; Du, D. Y.; Guan, W.; Bo, X. J.; Li, Y. F.; Guo, L. P.; Su, Z. M.; Wang, Y. Y.; Lan, Y. Q.; Zhou, H. C. Ultrastable Polymolybdate-Based Metal Organic Frameworks as Highly Active Electrocatalysts for Hydrogen Generation from Water. *J. Am. Chem. Soc.* **2015**, *137* (22), 7169–7177.
- (19) Islamoglu, T.; Goswami, S.; Li, Z.; Howarth, A. J.; Farha, O. K.; Hupp, J. T. Postsynthetic Tuning of Metal-Organic Frameworks for Targeted Applications. *Acc. Chem. Res.* **2017**, *50* (4), 805–813.
- (20) Rogge, S. M. J.; Bavykina, A.; Hajek, J.; Garcia, H.; Olivares-Suarez, A. I.; Sepulveda-Escribano, A.; Vimont, A.; Clet, G.; Bazin, P.; Kapteijn, F.; Daturi, M.; Ramos-Fernandez, E. V.; Llabres i Xamena, F. X.; Van Speybroeck, V.; Gascon, J. Metal-organic and covalent organic frameworks as single-site catalysts. *Chem. Soc. Rev.* **2017**, *46* (11), 3134–3184.
- (21) Qin, J. S.; Du, D. Y.; Li, M.; Lian, X. Z.; Dong, L. Z.; Bosch, M.; Su, Z. M.; Zhang, Q.; Li, S. L.; Lan, Y. Q.; Yuan, S.; Zhou, H. C. Derivation and Decoration of Nets with Trigonal-Prismatic Nodes: A Unique Route to Reticular Synthesis of Metal-Organic Frameworks. *J. Am. Chem. Soc.* **2016**, *138* (16), 5299–5307.
- (22) Tan, Y. X.; Wang, F.; Zhang, J. Design and synthesis of multifunctional metal-organic zeolites. *Chem. Soc. Rev.* **2018**, *47* (6), 2130–2144.
- (23) Wang, C.; Xie, Z.; deKrafft, K. E.; Lin, W. Doping metal-organic frameworks for water oxidation, carbon dioxide reduction, and organic photocatalysis. *J. Am. Chem. Soc.* **2011**, *133* (34), 13445–13454.
- (24) Sun, D.; Fu, Y.; Liu, W.; Ye, L.; Wang, D.; Yang, L.; Fu, X.; Li, Z. Studies on photocatalytic CO(2) reduction over NH₂-Uio-66(Zr) and its derivatives: towards a better understanding of photocatalysis on metal-organic frameworks. *Chem. - Eur. J.* **2013**, *19* (42), 14279–14285.
- (25) Xu, H. Q.; Hu, J.; Wang, D.; Li, Z.; Zhang, Q.; Luo, Y.; Yu, S. H.; Jiang, H. L. Visible-Light Photoreduction of CO₂ in a Metal-Organic Framework: Boosting Electron-Hole Separation via Electron Trap States. *J. Am. Chem. Soc.* **2015**, *137* (42), 13440–13443.

- (26) Lee, Y.; Kim, S.; Kang, J. K.; Cohen, S. M. Photocatalytic CO₂ reduction by a mixed metal (Zr/Ti), mixed ligand metal-organic framework under visible light irradiation. *Chem. Commun.* **2015**, 51 (26), 5735–5738.
- (27) Chen, D.; Xing, H.; Wang, C.; Su, Z. Highly efficient visible-light-driven CO₂ reduction to formate by a new anthracene-based zirconium MOF via dual catalytic routes. *J. Mater. Chem. A* **2016**, 4 (7), 2657–2662.
- (28) Tanabe, K. K.; Cohen, S. M. Postsynthetic modification of metal-organic frameworks—a progress report. *Chem. Soc. Rev.* **2011**, 40 (2), 498–519.
- (29) Deria, P.; Mondloch, J. E.; Karagiari, O.; Bury, W.; Hupp, J. T.; Farha, O. K. Beyond post-synthesis modification: evolution of metal-organic frameworks via building block replacement. *Chem. Soc. Rev.* **2014**, 43 (16), 5896–5912.
- (30) Yuan, S.; Qin, J. S.; Lollar, C. T.; Zhou, H. C. Stable Metal-Organic Frameworks with Group 4 Metals: Current Status and Trends. *ACS Cent. Sci.* **2018**, 4 (4), 440–450.
- (31) Wu, J.; Pisula, W.; Mullen, K. Graphenes as potential material for electronics. *Chem. Rev.* **2007**, 107 (3), 718–747.
- (32) Ong, W. J.; Tan, L. L.; Ng, Y. H.; Yong, S. T.; Chai, S. P. Graphitic Carbon Nitride (g-C₃N₄)-Based Photocatalysts for Artificial Photosynthesis and Environmental Remediation: Are We a Step Closer To Achieving Sustainability? *Chem. Rev.* **2016**, 116 (12), 7159–7329.
- (33) Narita, A.; Wang, X. Y.; Feng, X.; Mullen, K. New advances in nanographene chemistry. *Chem. Soc. Rev.* **2015**, 44 (18), 6616–6643.
- (34) Lee, J.; Kalin, A. J.; Wang, C.; Early, J. T.; Al-Hashimi, M.; Fang, L. Donor–acceptor conjugated ladder polymer via aromatization-driven thermodynamic annulation. *Polym. Chem.* **2018**, 9 (13), 1603–1609.
- (35) Vermeulen, N. A.; Karagiari, O.; Sarjeant, A. A.; Stern, C. L.; Hupp, J. T.; Farha, O. K.; Stoddart, J. F. Aromatizing Olefin Metathesis by Ligand Isolation inside a Metal-Organic Framework. *J. Am. Chem. Soc.* **2013**, 135 (40), 14916–14919.
- (36) Alezi, D.; Spanopoulos, I.; Tsangarakis, C.; Shkurenko, A.; Adil, K.; Belmabkhout, Y.; O’Keeffe, M.; Eddaoudi, M.; Trikalitis, P. N. Reticular Chemistry at Its Best: Directed Assembly of Hexagonal Building Units into the Awaited Metal-Organic Framework with the Intricate Polybenzene Topology, pbz-MOF. *J. Am. Chem. Soc.* **2016**, 138 (39), 12767–12770.
- (37) Scholl, R.; Seer, C. *Liebigs Ann. Chem.* **1912**, 394, 111.
- (38) Wu, J.; Watson, M. D.; Mullen, K. The versatile synthesis and self-assembly of star-type hexabenzocoronenes. *Angew. Chem., Int. Ed.* **2003**, 42 (43), 5329–5333.
- (39) Spek, A. L. Single-crystal structure validation with the program PLATON. *J. Appl. Crystallogr.* **2003**, 36 (1), 7–13.
- (40) Thompson, C. M.; Li, F.; Smaldone, R. A. Synthesis and sorption properties of hexa-(peri)-hexabenzocoronene-based porous organic polymers. *Chem. Commun.* **2014**, 50 (46), 6171–6173.
- (41) Karunatilake, A. A. K.; Chang, J.; Thompson, C. M.; Nguyen, C. U.; Nguyen, D. Q.; Rajan, A.; Sridharan, A.; Vyakaranam, M.; Adegboyega, N.; Kim, S. J.; Smaldone, R. A. Hexaphenylbenzene and hexabenzocoronene-based porous polymers for the adsorption of volatile organic compounds. *RSC Adv.* **2016**, 6 (70), 65763–65769.
- (42) Bichoutskaia, E.; Suyetin, M.; Bound, M.; Yan, Y.; Schröder, M. Methane Adsorption in Metal–Organic Frameworks Containing Nanographene Linkers: A Computational Study. *J. Phys. Chem. C* **2014**, 118 (29), 15573–15580.
- (43) Maeda, K.; Sekizawa, K.; Ishitani, O. A polymeric-semiconductor–metal-complex hybrid photocatalyst for visible-light CO₂ reduction. *Chem. Commun.* **2013**, 49 (86), 10127–10129.
- (44) Sun, D.; Liu, W.; Qiu, M.; Zhang, Y.; Li, Z. Introduction of a mediator for enhancing photocatalytic performance via post-synthetic metal exchange in metal-organic frameworks (MOFs). *Chem. Commun.* **2015**, 51 (11), 2056–2059.